Available online at www.sciencedirect.com
ScienceDirect
Journal of Catalysis 253 (2008) 303–311
JOURNAL OF CATALYSIS
www.elsevier.com/locate/jcat

CO multipulse TAP studies of 2% Pt/CeO_2 catalyst: Influence of catalyst pretreatment and temperature on the number of active sites observed

S.O. Shekhtman, A. Goguet, R. Burch, C. Hardacre *, N. Maguire

CenTACat, School of Chemistry and Chemical Engineering, Queen's University Belfast, Belfast BT9 5AG, Northern Ireland, UK

Received 5 July 2007; revised 8 October 2007; accepted 30 October 2007

Abstract

CO multipulse temporal analysis of products (TAP) experiments were used to characterize a ceria-supported platinum catalyst after various oxidative and reductive pretreatments using O_2, H_2O, CO_2, and H_2. Based on the amount of CO consumed, using the final CO-saturated catalyst composition as the common state point, the oxidatively pretreated catalyst could be described using a general scale. From a kinetic analysis of the CO multipulse responses, two kinetic regimes corresponding to two types of active sites could be identified. As the temperature was raised, the number of the most active sites did not change while the amount of the less active site increased. Comparison of the number of active sites determined from the TAP data reported herein with that determined by a previous steady-state isotope transient kinetic analysis experiment showed excellent agreement. This correlation indicates that the (very fast response) TAP experiments can provide information regarding the number and type of active sites that are relevant to a catalyst under real reaction conditions.

Keywords: TAP; Catalyst; Characterization; Ceria; Platinum

1. Introduction

The development of hydrogen fuel cells is among the most promising of all of the future energy solutions, providing efficient power with little environmental impact. However, providing hydrogen in a form that has sufficient purity not to deactivate the fuel cell is a major challenge. The reforming of hydrogen-rich fuels, including from renewable sources, is of major importance [1–4]. Such a reforming process involves a catalytic water–gas shift (WGS) step, which converts water into hydrogen while also removing CO, a poison for the fuel cell, forming CO_2; further removal of CO is achieved by selective oxidation (PrOx) without oxidation of the hydrogen [5]:

$$CO + H_2O \rightleftarrows CO_2 + H_2. \quad (1)$$

Recent studies have shown that noble metals (e.g., Pt, Au) supported on CeO_2 are promising low-temperature catalysts for these reactions [6–13]. However, there a number of conflicting reaction mechanisms by which the WGS and the PrOx reactions proceed [14–25]. These may be split into two broad themes, a redox process whereby the reactants oxidize and reduce the surface sequentially and an intermediate-derived process involving the formation of a surface species such as carboxylate, carbonate, or formate. Burch has recently proposed that both mechanisms may operate over the same catalyst for the WGS reaction with the reaction conditions determining the dominant route [9].

Over the last two decades, the temporal analysis of products (TAP) technique, developed by Gleaves and co-workers [26,27], has been successfully applied to non-steady-state kinetic characterization and investigation of reaction mechanisms of model and multicomponent industrial catalysts [28]. The TAP technique provides an opportunity to control the catalyst composition such that it does not change significantly during a single-pulse experiment because there are far fewer molecules pulsed than surface active sites/species. Furthermore, the catalyst state may be changed incrementally by exposing the catalyst to multiple pulses of gas [29].

In traditional approaches to the characterization of active sites, the sites are quantified using separate probe mole-

* Corresponding author.
E-mail address: c.hardacre@qub.ac.uk (C. Hardacre).

0021-9517/$ – see front matter
doi:10.1016/j.jcat.2007.10.028

cule adsorption experiments, for example, in calculation of the turnover frequency. In a multipulse TAP experiment, the amount of reactant consumed (analogous to an adsorption experiment) and the amount of product formed (characteristic of active surface species) in each single-pulse experiment are measured. These amounts are added from pulse-to-pulse to characterize the catalyst composition before each pulse [29]. On the completion of the multipulse experiment (i.e., when no further reaction is occurring), the total amount of the reactant consumed and product formed are determined; this is analogous to the uptake. An important advantage of the multipulse TAP experiment is that it allows measurement of a gradual change in the number of active sites/species as well as a change in the overall activity associated with the remaining sites. Thus, in a multipulse experiment it is possible to view the complete dependence of catalyst activity as a function of the amount of available active sites. A detailed analysis of this dependence allows the sites to be distinguished kinetically with respect to how rapidly the activity changes (e.g., decreases) as each site is taken up.

This paper provides the first description of how this methodology may be applied to multipulse TAP data. Such a multipulse experiment is particularly informative when combined with a thin-zone TAP reactor (TZTR) [30], which ensures uniformity in the catalyst zone [31]. The TZTR multipulse experiment allows state-by-state transient screening of the catalyst to be used to examine the active sites [32]. The catalyst state is continuously changed by a long multipulse experiment and probed kinetically by each single-pulse TAP experiment. A complete characterization of the catalyst using this methodology involves quantification/scaling of all catalyst states based on the amount of consumed molecules (e.g., according to reduction or oxidation), followed by understanding of the observed single-pulse kinetics versus this scale of catalyst state.

The present work used the TZTR multipulse experimental methodology to characterize the active sites for CO conversion on a Pt/CeO_2 catalyst studied previously using TAP for the reverse WGS reaction [33]. CO was used as a probe molecule in multipulse experiments performed as a function of temperature and normal pressure catalyst pretreatment under O_2, H_2, CO_2, and H_2O. The characterization shows the presence of two distinct sites, the numbers of which are strongly determined by the catalyst state.

2. Experimental

The 2% Pt/CeO_2 catalyst, provided by Johnson Matthey, had a BET surface area of 180 $m^2\,g^{-1}$ and a platinum dispersion of 17%. The metal dispersion was measured by H_2 chemisorption; note that the dispersion was measured at $-80\,^{\circ}C$, to minimize the potential spillover of H_2 onto the support [34]. This corresponds to a concentration of surface platinum atoms of $\sim 2 \times 10^{-8}$ mol mg_{cat}^{-1}. All gases were >99.9% purity and were supplied by BOC. Double-distilled deionized water (18.2 MΩ) was used. Before each reaction, the catalyst was activated under flowing 20% oxygen in nitrogen for 1 h.

The TAP pulse-response experiments were performed in a TAP-I reactor (Autoclave Engineers) using a stainless steel microreactor (41 mm long and 5.5 mm i.d.). In all of the experiments, the TZTR method was used where the reactor was packed with 2–3 mg of catalyst sandwiched between two 500 mg beds of silicon carbide. All particles were 250–450 μm in size. The reactor temperature was measured by a thermocouple positioned in the center of the catalyst bed. Reactants and products were recorded using a UTI 100C quadrupole mass spectrometer with a total collection time of 10 s. Each pulse comprised a 1:1 mix of ^{13}CO and argon. ^{13}CO was used to eliminate the influence of the high background observed at an AMU of 28 as part of the residual gas atmosphere. Masses at AMUs of 29, 40, and 45 were followed in the TAP transient mode. A typical multipulse experiment comprised >6000 pulses. The characteristic single-pulse responses were obtained by averaging a number of responses, varying from 2 responses at the beginning of the experiment to 10 responses at the end of the multipulse experiment. In the entire multipulse experiment reported, pulse intensity was determined from the monitored argon response intensity (which gradually changed during the experiment) and the pressure drop in the pulse chamber.

The following procedure was used for all experiments:

1. Pretreatment of the catalyst by exposing it to different gases at 1 atm pressure. Four different pretreatments were investigated:
   - I. 20% O_2 flow at 300 °C for 1 h.
   - II. 20% O_2 flow at 300 °C for 1 h, followed by flowing H_2 at 300 °C for 1 h, followed by 10% H_2O flow at 300 °C for 1 h.
   - III. 20% O_2 flow at 300 °C for 1 h, followed by flowing H_2 at 300 °C for 1 h, followed by 100% CO_2 flow at 300 °C for 1 h.
   - IV. 20% O_2 flow at 300 °C for 1 h, followed by flowing H_2 at 300 °C for 1 h.
2. Evacuation of the reactor to 10^{-6} Torr.
3. Vacuum pulse-response TAP experiments using CO multipulses at the desired temperature.

The exit flow rate time dependence for each reactant/product and inert was determined using standard mass spectrometry fragmentation patterns and sensitivity factors normalized to argon.

3. Results and discussion

3.1. Influence of pretreatment

This section reports the results of CO multipulse experiments over various catalysts that underwent different pretreatments. During each multipulse experiment, the intensity of the CO responses increased (i.e., CO consumption decreased) with increasing pulse number; ultimately reaching a point at which CO molecules were no longer consumed by the catalyst. The single-pulse CO conversion was determined as the ratio between the amount of CO consumed and amount of CO injected

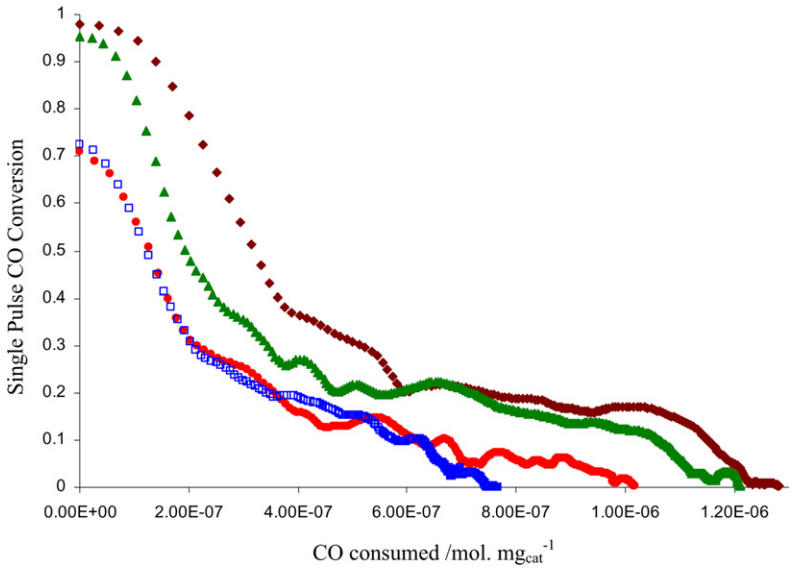

Fig. 1. Single-pulse CO conversion variation with respect to the amount of consumed CO prior to each CO pulse at 300 °C as a function of O_2 (◆), H_2O (▲), CO_2 (●), and H_2 (□) catalyst pretreatments.

into the reactor in a single-pulse. The change in catalyst composition in a multipulse experiment was characterized by the amount of CO molecules consumed by the catalyst before each pulse in the series (calculated from a single-pulse CO consumption and pulse intensity monitored by the argon responses). This scale is much more informative than the pulse number, because both pulse intensity and CO consumption change during a TAP multipulse experiment. Thus, the change in catalyst composition varies significantly from pulse to pulse, and the scale-based on the amount of CO consumed explicitly quantifies this change.

Fig. 1 shows typical single-pulse CO conversion profiles as a function of the amount of CO consumed before each CO pulse over 2 mg of pretreated 2% Pt/CeO_2 catalyst in a CO multipulse TAP experiment at 300 °C. Four profiles are shown to illustrate the influence of the normal pressure pretreatments (I–IV). The total amount of CO consumed in the full multipulse experiment, the first pulse activity, and the profiles generally are different for the different catalyst pretreatments. These results indicate that, as expected, different normal pressure pretreatment and evacuation regimes had different effects on catalyst surface composition.

Despite these differences, a more informative graphical representation of conversion profiles was found. In this representation, the pulse at which no more CO was consumed was used as a common end point, corresponding to the point at which the catalyst was saturated with CO in all four cases. Fig. 2 presents the same (as in Fig. 1) single-pulse CO conversion profiles plotted using this common end point. This figure clearly shows that the single-pulse CO conversion observed in multipulse experiments over differently preoxidized catalysts (i.e., using O_2, H_2O, and CO_2) follows a single curve when plotted against this new general scale. Within this general scale, a different oxidizing pretreatment is reflected as a merely different starting point on the general curve according to total CO consumption for each pretreatment, indicating that I (O_2) > II (H_2O) > III (CO_2). The maximum amount of CO consumption was found after the oxygen treatment, corresponding to 1.28×10^{-6} mol mg_{cat}^{-1}, whereas after the H_2O treatment, consumption was lower, by $\sim 5 \times 10^{-8}$ mol mg_{cat}^{-1}. This difference is within the range of the number of surface platinum atoms, possibly indicating that H_2O oxidizes the same sites as O_2 except those sites associated with platinum atoms. Compared with the O_2 pretreatment, CO_2 pretreatment resulted in lower CO consumption. The difference of 2.3×10^{-7} mol mg_{cat}^{-1} is clearly greater than the number of platinum atoms. In addition, the first pulse activity dropped by ~25% compared with the oxygen treatment case. For all oxidation pretreatments, a small amount of CO_2 (10–15% of CO consumed) was observed in the form of a broad feature indicating slow reaction/desorption.

As discussed below, most of the CO is consumed during the reaction to form a stable surface intermediate, such as surface carbonate. Therefore, although CO_2 pretreatment will reoxidize the catalyst surface after reduction, it also will produce surface carbonates, which may block the active sites and cause lower first pulse activity and a decrease in total CO consumption compared with either O_2 or H_2O pretreatment. In summary, the oxygen pretreatment results in a completely oxidized catalyst surface, both platinum and support; the water oxidizes only the oxide support, and not the metal sites as follows from difference; and the CO_2 pretreatment not only oxidizes the oxide support, but also blocks some other active sites through the formation of surface carbonates.

In contrast to the oxidative treatments, after H_2 pretreatment only, no detectable amount of CO_2 produced was observed, although a significant CO consumption activity for the initial pulses was seen (Fig. 1). This is likely due to CO disproportionation, with the CO_2 formed during the reaction being trapped through strong readsorption on the reduced ceria [35]. The conversion profile for H_2 pretreatment did not follow the general curve as for the oxidized catalyst (Fig. 2). With an increasing

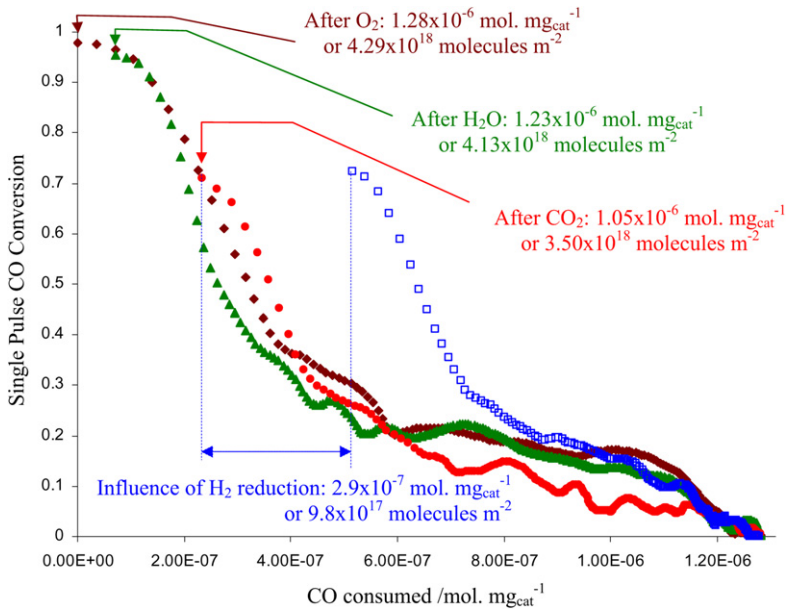

Fig. 2. Single-pulse CO conversion variation with respect to the amount of consumed CO prior to each CO pulse at 300 °C as a function of O_2 (◆), H_2O (▲), CO_2 (●), and H_2 (□) catalyst pretreatments. Compared with the traces shown in Fig. 1, the curves have been shifted in order for all the profiles to have a common ending point providing evidence of a general scale over a range pretreatments.

number of CO pulses, the activity decreased, but for the reduced catalyst, fewer pulses of CO were required before the catalyst activity reached zero. This finding was expected, because the capacity to adsorb/react with CO after a reductive treatment will decrease due to removal of labile oxygen from the support. Interestingly, the amount of CO consumed far exceeded the number of exposed Pt atoms (CO/Pt ∼ 40) which is consistent with previous observations made for this catalyst that the carbon produced through CO disproportionation is unlikely to be located only on the Pt [36]. In this case the disproportionation either occurs on the metal and part of the carbon spills over the support, or at least part of the disproportionation reaction occurs directly on the ceria support.

We analyzed single-pulse responses using moment formalism as described in detail previously [29]. According to this theory, each moment of observed response (M_0, M_1, M_2) allows the determination of only one independent kinetic parameter (R_0, R_1, R_2), called the primary kinetic coefficient. For the TZTR CO multipulse responses, the zeroth coefficient, R_0, is calculated from the zeroth moment, M_0, as

$$R_0 = \frac{1 - M_0}{\tau_{cat} M_0}, \tag{2}$$

R_0 has the dimension of reciprocal time (s) and represents an apparent rate constant of CO consumption.

The first coefficient, R_1, is calculated from the first moment, M_1, as

$$R_1 = \frac{M_1}{\tau_{cat} M_0^2} - \tau_{in}\left(\frac{1}{\tau_{cat}} + \frac{R_0}{3}\right). \tag{3}$$

R_1 is dimensionless and represents CO apparent "intermediate-gas" constant, which relates gaseous and adsorbed CO.

The second coefficient, R_2, is calculated from the second moment, M_2, as

$$-R_2 = \frac{M_2}{2\tau_{cat} M_0^2} - \frac{M_1^2}{\tau_{cat} M_0^3} + \frac{\tau_{in}}{6}\left(\frac{\tau_{in} R_0}{5} + 2R_1 + \frac{\tau_{in}}{\tau_{cat}}\right), \tag{4}$$

where R_2 has the dimension of time (s) and describes CO apparent time delay on the catalyst surface.

$$\tau_{cat} = \frac{L_r L_{cat}}{2D_{in}}$$

is the residence time in the catalyst zone, and

$$\tau_{in} = \frac{\varepsilon_{in} L_r^2}{2D_{in}}$$

is the residence time in inert zones. The explicit expressions (2)–(4) have been recently detailed by Shekhtman et al. [37].

The fact that R_1 and R_2 calculated for CO were >0 throughout the entire multipulse experiment suggested a holdup of the CO in the reactor bed (as proposed in [29]). The same conclusion follows from the comparison of typical argon and CO responses observed at the end of a multipulse experiment shown in Fig. 3 where it is clear that the CO response is broader. This indicates that the CO molecule adsorbs reversibly during the multipulse experiments. The fact that the CO consumption is not balanced by the CO_2 release indicates that the adsorbed CO also transforms into a long-lived surface intermediate. These conclusions lead to the following mechanism for CO adsorption/desorption and reaction:

$$CO \underset{k_d}{\overset{k_a}{\rightleftarrows}} CO_{ads},$$

$$CO_{ads} \xrightarrow{k_{trans}} \text{Intermediate}. \tag{5}$$

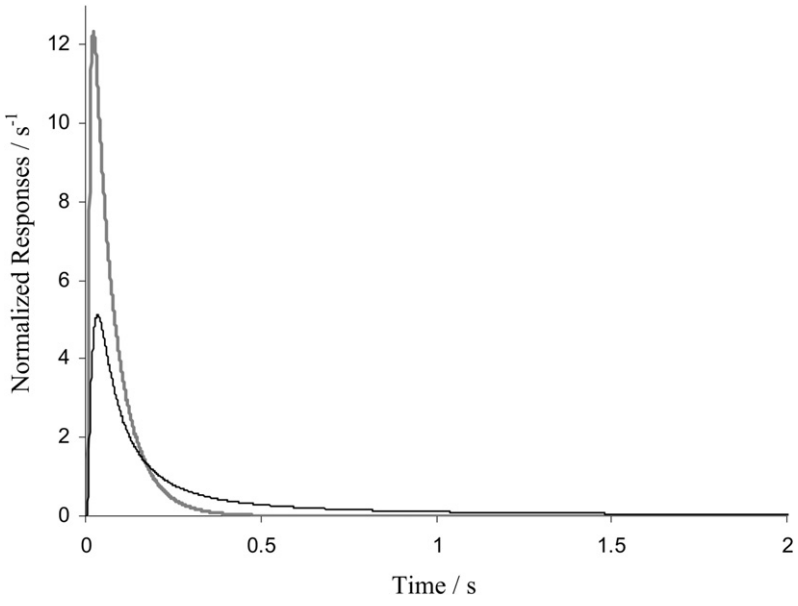

Fig. 3. Typical normalized argon (grey thick) and CO (black) responses observed near the end of multipulse experiment.

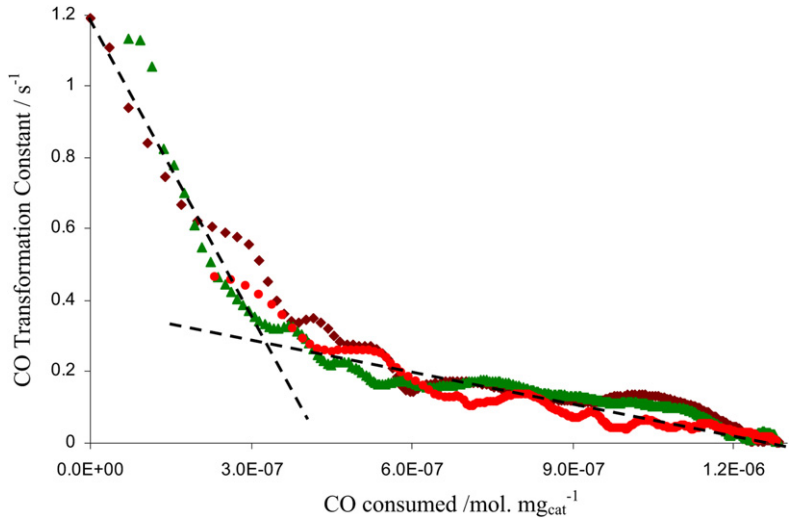

Fig. 4. Rate constant of surface CO transformation versus the amount of consumed CO prior to each CO pulse at 300 °C as a function of O_2 (◆), H_2O (▲), and CO_2 (●) catalyst pretreatments. Dashed lines indicate two linear regimes.

The rate constants of these elementary steps (i.e., for CO adsorption, desorption, and surface reaction) were determined from the primary kinetic coefficients (R_0, R_1, and R_2) using relationships reported in Table 1 (reversible adsorption + irreversible reaction) of [29]. In particular,

$$\frac{1}{k_{\text{trans}}} = \frac{R_1}{R_0} - \frac{R_2}{R_1} \quad \text{and} \quad k_{\text{d}} = \frac{k_{\text{trans}} R_1^2}{R_0 R_2}. \tag{6}$$

As reported previously in [33], the desorption constant remained around 1.5 s^{-1} during all multipulse experiments while the transformation constant varied. As found in Fig. 2, the single-pulse CO conversion observed in the multipulse experiments over differently preoxidized catalysts followed a single curve when plotted against the general scale. Fig. 4 shows the surface transformation constant plotted against the general scale. Clearly, k_{trans} observed over differently preoxidized catalysts also follows a single curve. This curve may be treated as a combination of two linear relationships that are indicative of two types of active sites, as indicated by the lines shown in Fig. 4.

3.2. Influence of reaction temperature

The variation in CO conversion dependence versus the amount of CO consumed for the oxygen-pretreated catalyst as a function of reaction temperature was measured to determine the influence of temperature on of the number and activity of different active sites. Oxygen pretreatment was chosen because it provides the most extensive multipulse dependence, as discussed in the previous section. In all the experiments, the normal pressure oxidation and evacuation were conducted at 300 °C to produce a similar catalyst surface. Thereafter, the

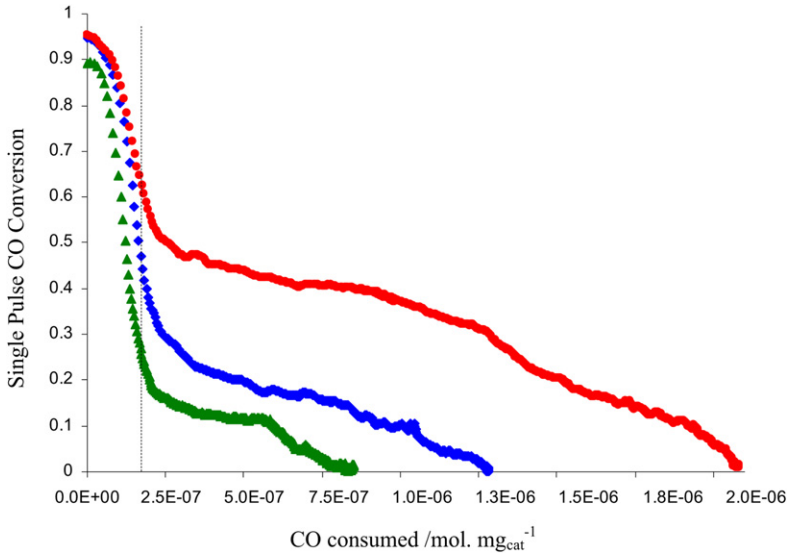

Fig. 5. The single-pulse CO conversion versus the amount of CO consumed prior to each CO pulse observed for oxygen pretreated catalyst at 250 (▲), 300 (◆), and 350 °C (●).

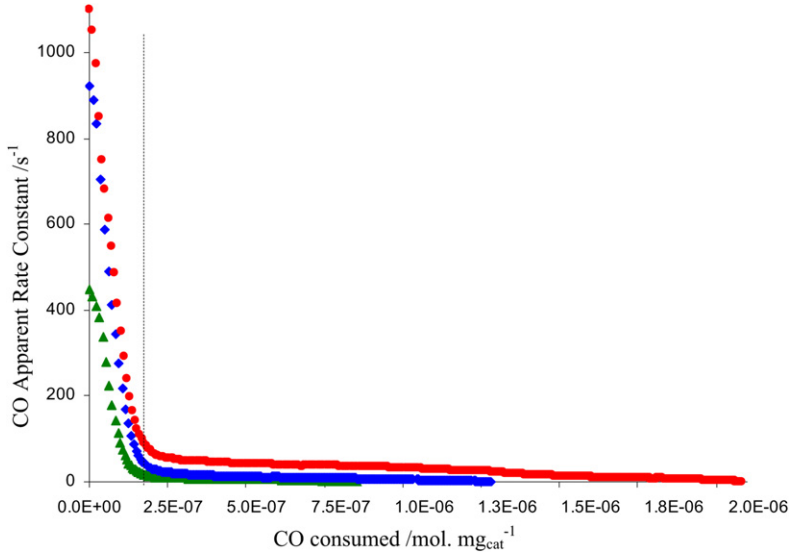

Fig. 6. CO apparent rate constant versus the amount of CO consumed per mg of catalyst for the oxygen pretreated catalyst at 250 (▲), 300 (◆), and 350 °C (●).

temperature was adjusted to the desired value under vacuum before the corresponding CO multipulse.

Figs. 5 and 6 show the single-pulse CO conversion and CO apparent rate constant [i.e., R_0 calculated from Eq. (2)], as a function of the amount of CO consumed before the corresponding CO pulse observed at 250, 300, and 350 °C over 3 mg of catalyst, respectively. Good consistency was found for the total amount of CO consumed in the multipulse experiment and the kinetic characteristics at 300 °C between 2 and 3 mg of catalyst, indicating that the TZTR remained well defined. From Fig. 5, in general, the single-pulse conversion increased with temperature throughout the entire multipulse experiment, as expected. Furthermore, the total amount of CO consumed in a completed multipulse experiment also increased with temperature, possibly indicating increasingly deeper reduction of the support with increasing temperature. Irrespective of the temperature, each curve is again characterized by two regions, with the transition point between the regions denoted by a dashed line in Fig. 5. The amount of CO consumed within the region in which the conversion decreased most rapidly did not change with the temperature, remaining at $\sim 1.5 \times 10^{-7}$ mol $\mathrm{mg}_{\mathrm{cat}}^{-1}$. In contrast, in the second region, the amount of CO consumed increased with increasing temperature, leading to the observation that the overall amount of CO consumed also increased. A similar pattern occurred for the apparent rate constant (R_0) shown in Fig. 6. The apparent rate constant decreased rapidly for the first 1.5×10^{-7} mol of CO consumed, then decreased much more gradually to zero activity. Again, the two regions found in Fig. 5 are clearly shown in Fig. 6.

According to a general concept of active sites, the rate constant should be proportional to the amount of available sites and should decrease linearly as these sites are taken up. The

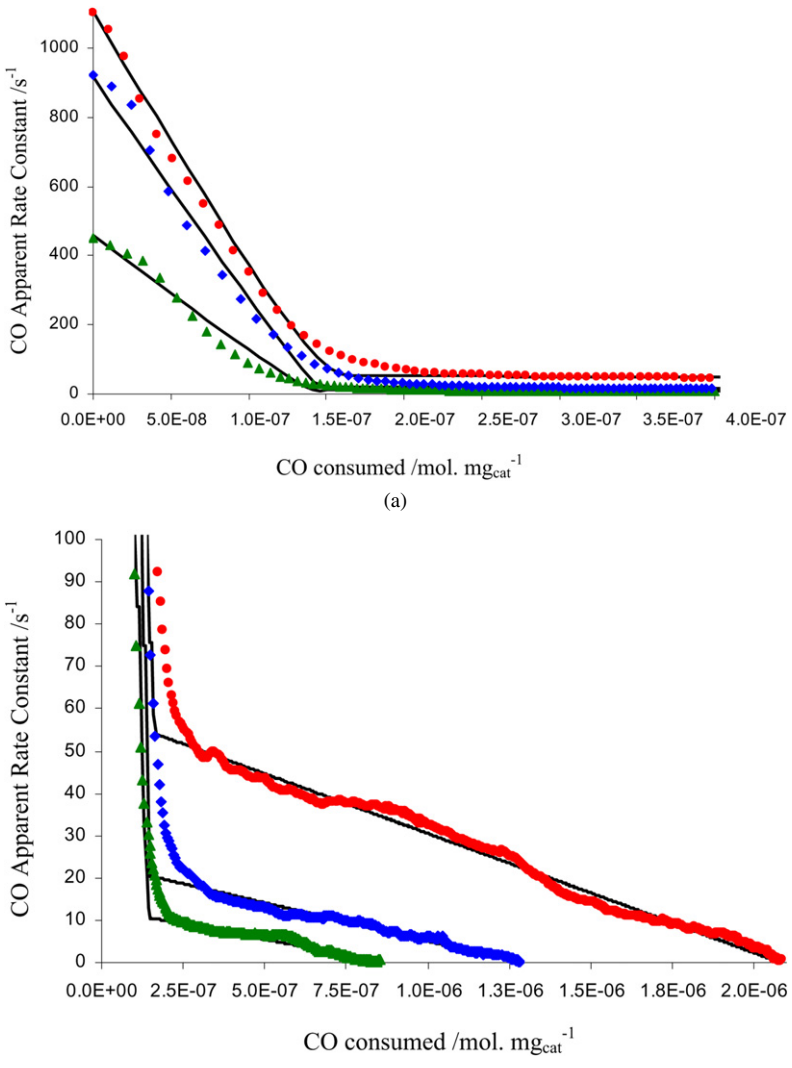

Fig. 7. CO apparent rate constants observed in multipulse experiments at 250 (▲), 300 (◆), and 350 °C (◆) and rate constants, k_{model}, calculated using the model described by Eq. (2) (straight lines) as a function of the CO consumed. The x-axis of plot (b) is expanded compared with plot (a) to illustrate the fit in the fast and slow change regions, respectively.

decrease in the CO apparent rate constant may be fitted by a combination of two linear functions at all three temperatures, but not by a single linear or quasi-linear function. The linear decrease of the rate constant with CO consumption is indicative of domination of a single type of active site when each CO molecule takes up an active site while being consumed. The different slopes of the linear dependency indicate different activity for the sites. Consequently, these two regions can be associated with different active sites. The overall activity can be modeled as a weighted average of the rate constants for an individual site and the number of sites available,

$$k_{\text{model}} = k_1(1-\theta_1) + k_2(1-\theta_2), \tag{7}$$

where $\theta_1 = N_{\text{CO},1}/N_1$ is the coverage of CO over more active sites, N_1; $\theta_2 = N_{\text{CO},2}/N_2$ is the coverage of CO over less active sites, N_2; and k_1 and k_2 represent the activity of corresponding sites.

With CO consumption, both $N_{\text{CO},1}$ and $N_{\text{CO},2}$ increase from zero to maximum values (N_1, N_2) over the entire multipulse experiment, and the amount of CO consumed in each pulse is measured. The amount of CO consumed that reacts with sites 1 and 2 is proportional to the activity of the sites [i.e., $k_1(1-\theta_1)$ or $k_2(1-\theta_2)$, respectively], as calculated for the previous pulse. The pulse-to-pulse evolution of model k_{model} [Eq. (7)] was then calculated from the observed single-pulse CO consumption and fitted to experimentally observed kinetic dependencies (Fig. 6) using least squares regression. Fig. 7 shows this fit, indicating that the reaction data is consistent with a two-site model (but not a single-site model) in which the sites of very different activity work independently in a parallel manner. Significant differences in activity clearly separate the contribution of each kind of site into two quasi-linear regions. The values of the fitting parameters [i.e., the numbers (N_1, N_2) and activity (k_1, k_2) of the two kinds of active sites] are given in Table 1. Table 1 also compares the equivalent site density determined using a steady-state isotope transient kinetic analysis (SSITKA) experiment at 225 °C [20]. Similar values for the calculated amounts of two distinct kinds of active sites were found for the TAP

Table 1
Fitting parameters of the two site model shown in Eq. (7) associated with the low and high activity sites

Temperature (°C)	More active sites		Less active sites	
	Number, N_1 (mol mg_{cat}^{-1})	Kinetic constant, k_1 (s^{-1})	Number, N_2 (mol mg_{cat}^{-1})	Kinetic constant, k_2 (s^{-1})
250	1.30×10^{-7}	450	0.75×10^{-6}	11
300	1.35×10^{-7}	900	1.15×10^{-6}	21
350	1.33×10^{-7}	1050	1.95×10^{-6}	55
	Activation energy: 23 kJ mol^{-1}		Activation energy: 44 kJ mol^{-1}	
SSITKA data at 225 °C [20]	CO precursor: 2.2×10^{-7} mol mg_{cat}^{-1}		CO_2 precursor: 8.4×10^{-7} mol mg_{cat}^{-1}	

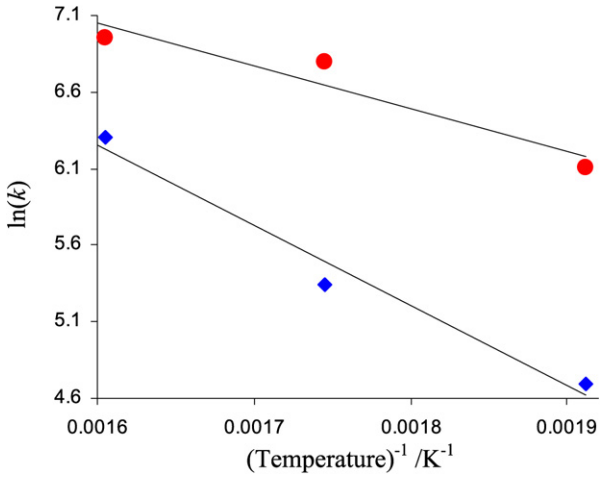

Fig. 8. Arrhenius plot for the rate constants k_1 (●) and $k_2 \times 10$ (◆) determined from the fitting using Eq. (2) for the high and low activity sites, respectively.

vacuum multipulse experiments and the reverse WGS SSITKA study [33]. From the SSITKA data, the amounts of gaseous CO and CO_2 released by the catalyst surface after the isotope switch were determined to be $N_{CO} = 2.2 \times 10^{-7}$ mol mg_{cat}^{-1} and $N_{CO_2} = 8.4 \times 10^{-7}$ mol mg_{cat}^{-1}, respectively, at 225 °C. The activity (k_1, k_2) of each site can be described by an Arrhenius dependence as shown in Fig. 8 with activation energies of 23 kJ mol^{-1} for the higher activity site and 44 kJ mol^{-1} for the lower activity site.

The thermal variation may be investigated by assigning the more active sites to those associated with the platinum particles (i.e., on both the metal and those in the close vicinity), because the number of these sites exceeds the amount of platinum atoms. The less active sites can be associated only with the support. This is consistent with an earlier observation made for this catalyst associating the most active sites with close proximity of the Pt particles [36]. These sites can be easily reduced and thus likely to show little temperature variation in the number of sites available. In contrast, sites further away from the metal are more difficult to reduce, resulting in a significant temperature variation. Interestingly, the fact that the two sites have different apparent activation barriers demonstrates that the lower-activity site will dominate at higher temperatures, resulting in a switch to a different reaction mechanism as a function of temperature. This is particularly relevant to the WGS reaction, for which a debate is ongoing as to whether an associative or a redox mechanism predominates. It is possible that both mechanisms occur and that only the temperature at which the reaction is performed governs which one predominates.

4. Conclusion

In this work, CO multipulse TAP experiments were performed to characterize the number and type of active sites on a Pt/CeO_2 CO oxidation/WGS catalyst. The influence of normal pressure pretreatment and reaction temperature were studied in detail. The influence of different normal pressure pretreatments was quantified based on the amount of CO consumed. The kinetic characteristics (e.g., conversion) observed over differently preoxidized catalysts followed a single curve when plotted using the final CO-saturated catalyst composition as the common state. Different pretreatments are represented as different starting points on this curve (indicating different levels of oxidation).

Based on kinetic data obtained at different temperatures, the catalyst was found to contain two distinct, independent sites each with significantly different activity. These sites were considered to be associated with the metal/metal-modified support and the support corresponding to high and low activity, respectively. The number of low activity sites was found to increase with temperature, whereas little temperature variation was seen for the higher-activity sites. The higher activity of each type of site followed an Arrhenius dependence, with higher activation energy for less-active sites. Good agreement was found between the TAP and SSITKA experiments, demonstrating that TAP experiments can provide information regarding the active sites relevant to a catalyst under real reaction conditions.

Acknowledgments

The authors thank Johnson Matthey for supplying the catalyst. Funding was provided by the EPSRC under the CARMAC project. A studentship (for N.M.) was provided by DEL.

References

[1] Y. Jamal, M.L. Wyszinski, Int. J. Hydrogen Energy 19 (1994) 557.
[2] M.A. Pena, J.P. Gomez, J.L.G. Fierro, Appl. Catal. A 144 (1996) 7.
[3] G. Maggio, S. Freni, S. Cavallaro, J. Power Sources 74 (1998) 17.
[4] A.N. Fatsikostas, D.I. Kondarides, X.E. Verykios, Chem. Commun. (2001) 851.
[5] J.M. Zalc, V. Sokolvskii, D.G. Löffler, J. Catal. 206 (2002) 169.
[6] Q. Fu, A. Weber, M. Flytzani-Stephanopoulos, Catal. Lett. 77 (2001) 87.

[7] S. Ricote, G. Jacobs, M. Milling, Y. Ji, P.M. Patterson, B.H. Davis, Appl. Catal. A 303 (2006) 35.
[8] D. Tibiletti, A. Amieiro-Fonseca, R. Burch, Y. Chen, J.M. Fisher, A. Goguet, C. Hardacre, P. Hu, A. Thompsett, J. Phys. Chem. B 109 (2005) 22553.
[9] R. Burch, Phys. Chem. Chem. Phys. 8 (2006) 5483.
[10] A.F. Ghenciu, Curr. Opin. Solid State Mater. Sci. 6 (2002) 389.
[11] H. Son, A.M. Lane, Catal. Lett. 76 (2001) 151.
[12] R. Farrauto, S. Hwang, L. Shore, W. Ruettinger, J. Lampert, T. Giroux, Y. Liu, O. Ilinich, Ann. Rev. Mater. Res. 33 (2003) 1.
[13] D. Duprez, J. Chim. Phys. Phys. Chim. Biol. 92 (1995) 1952.
[14] T. Bunluesin, R.J. Gorte, G.W. Graham, Appl. Catal. B 15 (1998) 107.
[15] R.J. Gorte, S. Zhao, Catal. Today 104 (2005) 18.
[16] T. Shido, Y. Iwasawa, J. Catal. 136 (1992) 493;
T. Shido, Y. Iwasawa, J. Catal. 141 (1993) 71.
[17] G. Jacobs, B.H. Davis, Appl. Catal. A 284 (2005) 31.
[18] G. Jacobs, S. Ricote, B.H. Davis, Appl. Catal. A 302 (2006) 14.
[19] F.C. Meunier, D. Tibiletti, A. Goguet, S. Shekhtman, C. Hardacre, R. Burch, Catal. Today 126 (2007) 143.
[20] A. Goguet, F.C. Meunier, D. Tibiletti, J.P. Breen, R. Burch, J. Phys. Chem. B 108 (2004) 20240.
[21] A. Wootsch, C. Descorme, D. Duprez, J. Catal. 225 (2004) 259.
[22] A. Trovarelli, Catal. Rev. Sci. Eng. 38 (1996) 439.
[23] O. Pozdnyakova, D. Teschner, A. Wootsch, J. Krohnert, B. Steinhauer, H. Sauer, L. Toth, F.C. Jentoft, A. Knop-Gericke, Z. Paal, R. Schlogl, J. Catal. 237 (2006) 1.
[24] O. Pozdnyakova, D. Teschner, A. Wootsch, J. Krohnert, B. Steinhauer, H. Sauer, L. Toth, F.C. Jentoft, A. Knop-Gericke, Z. Paal, R. Schlogl, J. Catal. 237 (2006) 17.
[25] A. Wootsch, C. Descorme, D. Duprez, J. Catal. 225 (2004) 259.
[26] J.T. Gleaves, J.R. Ebner, T.C. Kuechler, Catal. Rev. Sci. Eng. 30 (1988) 49.
[27] J.T. Gleaves, G.S. Yablonskii, P. Phanawadee, Y. Schuurman, Appl. Catal. A 160 (1997) 55.
[28] G.S. Yablonsky, M. Olea, G.B. Marin, J. Catal. 216 (2003) 120.
[29] S.O. Shekhtman, G.S. Yablonsky, J.T. Gleaves, R. Fushimi, Chem. Eng. Sci. 58 (2003) 4843.
[30] S.O. Shekhtman, G.S. Yablonsky, J.T. Gleaves, S. Chen, Chem. Eng. Sci. 54 (1999) 4371.
[31] S.O. Shekhtman, G.S. Yablonsky, Ind. Eng. Chem. Res. 44 (2005) 6518.
[32] S.O. Shekhtman, G.S. Yablonsky, J.T. Gleaves, R. Fushimi, Chem. Eng. Sci. 59 (2004) 5493.
[33] A. Goguet, S.O. Shekhtman, R. Burch, C. Hardacre, F.C. Meunier, G.S. Yablonsky, J. Catal. 237 (2006) 102.
[34] S. Bernal, F.J. Botana, J.J. Calvino, M.A. Cauqui, G.A. Jobacho, J.M. Pintado, J.M. Rodriguez-Izquierdo, J. Phys. Chem. 97 (1993) 4118.
[35] F.C. Meunier, D. Tibiletti, A. Goguet, D. Reid, R. Burch, Appl. Catal. A 289 (2005) 104.
[36] A. Goguet, F. Meunier, J.P. Breen, R. Burch, M.I. Petch, A. Faur Ghenciu, J. Catal. 226 (2004) 382.
[37] S.O. Shekhtman, N. Maguire, A. Goguet, R. Burch, C. Hardacre, Catal. Today 121 (2007) 255.